Shapley additive explanation on machine learning predictions of fatigue lifetimes in piston aluminum alloys under different manufacturing and loading conditions

Mahmood Matin, Mohammad Azadi
Faculty of Mechanical Engineering, Semnan University, Semnan, Iran
m_azadi@semnan.ac.ir, http://orcid.org/0000-0001-8686-8705

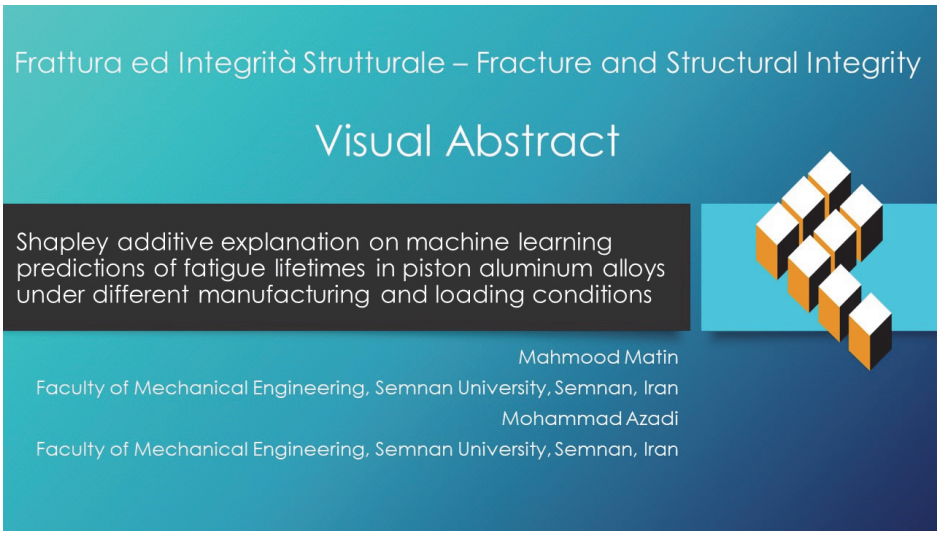

Citation: Matin, M., Azadi, M., Shapley additive explanation on machine learning predictions of fatigue lifetimes in piston aluminum alloys under different manufacturing and loading conditions, Frattura ed Integrità Strutturale, 68 (2024) 357-370.

Received: 06.01.2024
Accepted: 07.03.2024
Published: 11.03.2024
Issue: 04.2024

KEYWORDS. Machine learning, Bending fatigue, Lifetime estimation, Piston aluminum alloys, Shapley additive explanation.

INTRODUCTION

Aluminum-silicon alloys have been extensively utilized in internal combustion (IC) engines as a substitute for cast iron and steel components to decrease the weight, resulting in the reduction of emissions and fuel consumption [1]. The piston must be robust and durable to withstand thermomechanical fatigue while being lightweight and resistant to wear [2]. Considering the remarkable mechanical properties and lightness, aluminum alloys emerge as one of the best choices for piston manufacturing [3].

There are several approaches for predicting fatigue lifetimes. Sun and Shang [4] examined the fatigue lifetime estimation of tubular and notched specimens by employing the finite element method (FEM), compared to experimental data under multiaxial loading conditions. Shivachev and Myagkov [5] developed an ANSYS-based method to calculate the transient temperature and strain fields of a piston under different loads, with a focus on evaluating its fatigue lifetime. The fatigue lifetime estimation was executed with a linear regression modeling (LRM) [6] and the neural network technique [7]. Furthermore, Pearson correlation coefficient, permutation feature importance, and accumulated local effects were investigated for the sensitivity analysis of fatigue life modeling inputs [8]. For this objective, SHAP values, known as Shapley

Additive Explanations, provide a valuable method for determining the significance of each feature on output prediction. Moreover, numerous research studies have been performed using this approach in various fields, such as material engineering [9,10], environmental engineering [11], and mineral engineering [12].

Data science methods were employed to estimate the fatigue characteristics of aluminum alloys. In a study, Abdullatef et al. [13] assessed the accuracy of different machine learning (ML) and artificial intelligence (AI) approaches in predicting the fatigue lifetime of an aluminum alloy based on bending fatigue data. They compared artificial neural networks, support vector machines (SVM) with different kernels, extreme gradient boosting (XGBoost), random forest (RF), and additive neuro-fuzzy inference. They reported that for estimating the fatigue lifetime of 2090-T83 aluminum alloys, the neuro-fuzzy inference method was an accurate model, but XGBoost, due to its simple floating-point nature, was deemed the optimum and fastest one. Yasnii et al. [14] used ML approaches to analyze the fatigue fracture and load ratio effects on D16T aluminum alloys, achieving accurate predictions with the lowest error of 3.2% and 2.5%. Additionally, Lian et al. [15] utilized a dataset generated for plotting S-N (stress-life) curves for seven types of aluminum alloys. Firstly, using XGBoost, they investigated the effect of each element in the alloys to predict their fatigue lifetimes based on SHAP values, revealing that aluminum and magnesium had the most significant impact on the fatigue lifetime of the alloys. Secondly, they conducted feature engineering to identify the most influential feature on the fatigue lifetime estimation, utilizing SHAP values for this analysis. They reported that the Stussi feature (a functional attribute related to the fatigue lifetime) and $\sigma_{max}^{1.5}$ (the maximum stress with the power of 1.5) had the most significant impact on the fatigue lifetime of aluminum alloys. Matin and Azadi [16] estimated the transition fatigue lifetime of an aluminum alloy by utilizing unsupervised machine-learning modeling. Moreover, they cluster the S-N curves from high-cycle fatigue to low-cycle fatigue to show the influence of stress variation on fatigue lifetime. Azadi and Parast [17] investigated the effects of assumed inputs, consistent with those in this study, on rotational bending fatigue tests using regression models. In their findings, stress had the most impact on the fatigue lifetime with a score of 1, the fretting force with a score of 2, and the corrosion time with a score of 3. The results of the aforementioned studies emphasized the benefits of employing ML techniques, serving as an inspiration to extend the application of ML techniques to other research domains like the fatigue estimation of aluminum alloys. Moreover, a common sensitivity analysis cannot interpret a model with high variation, and it is not helpful for nonlinear variations. The motivation for this work could be the utilization of an accurate ML model with a precise interpretation, such as SHAP values. One of the extra motivations for employing ML approaches was the lack of a simple physical-based solution for the mentioned work [17].

Nowadays, researchers demonstrate that because of the variation in fatigue lifetime and the experimental nature of fatigue, physics-based ML models can estimate the fatigue problem better than traditional ML methods, achieving high accuracy with low-trained data [18,19]. However, the present work aims to propose the interpretation of the impact of certain binary and continuous physical features, demonstrating their effect on the estimation of fatigue lifetime and its logarithm value directly, without using feature engineering, constraint enforcement, hybrid models, or optimizers, as represented in the literature [20], to build higher accuracy models. Furthermore, a study demonstrated the effect of preprocessing methods and data normalization on the dataset used in this paper. It shows that employing preprocessing methods aligned with the physics of fatigue could enhance the performance of the models [21].

This work innovatively investigates the influence of various experimental and manufacturing factors on piston aluminum alloy specimens under rotational bending fatigue tests, utilizing ML techniques to assess their significance and interactions affecting fatigue lifetime values. It also introduces a novel approach to estimating the fatigue lifetime under the assumed conditions, particularly significant for the piston and automotive manufacturing industries.

RESEARCH METHODS

Experimental Dataset

This section explains the experimental dataset [17], which was utilized in the present work. Parast and Azadi [17] examined the performance of various standard specimens, following ISO-1143, for conducting corrosion fatigue (CF), pure fatigue (PF), and fretting fatigue tests (FF), under different inputs. Moreover, these specimens were fabricated with an alloy commercially known as AlSi12CuNiMg, which is commonly applicable in the piston manufacturing industry. The variables were as follows: the stress level (90-210 MPa), the existence of nanoparticles for the reinforcement (True or False), the presence of T6 heat treatment (True or False), the existence of lubrication (True or False), the pre-corrosion time in H2SO4 (0-200 hours), and the fretting force (0-20 N) [17]. These experiments involved six different parameters, and a dataset with 147 samples was generated, with the fatigue lifetime as the output. Tab. 1 briefly demonstrates the dataset used in this paper for 147 data points.

	Label	Units/Boolean	Min Value	Max Value	Mean
Features	Fretting Force	N	0	20	4.83
	Corrosion Time	hr	0	200	76.19
	Stress	MPa	90	210	158.57
	Nano-particle	Boolean	False	True	-
	Heat-treating	Boolean	False	True	-
	Lubrication	Boolean	False	True	-
Target	Fatigue lifetime	Cycle	500	1398100	77336

Table 1: The dataset in brief.

Fig. 1 illustrates the standard ISO-1143 specimens used in the rotational bending fatigue testing machine, within this experimental dataset [17]. Additionally, Fig. 2 depicts the rotational stress-controlled fatigue testing machine under bending loads and equipped with a fretting module [17].

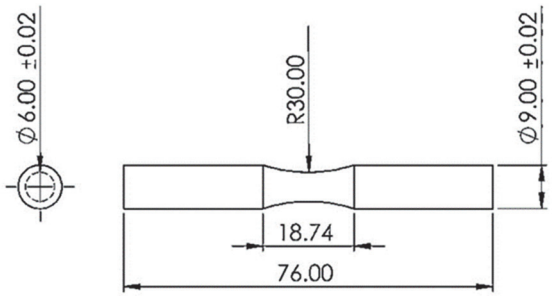

Figure 1: The shape and dimensions of specimens in the experimental dataset for the rotary bending fatigue test (units in mm) [17].

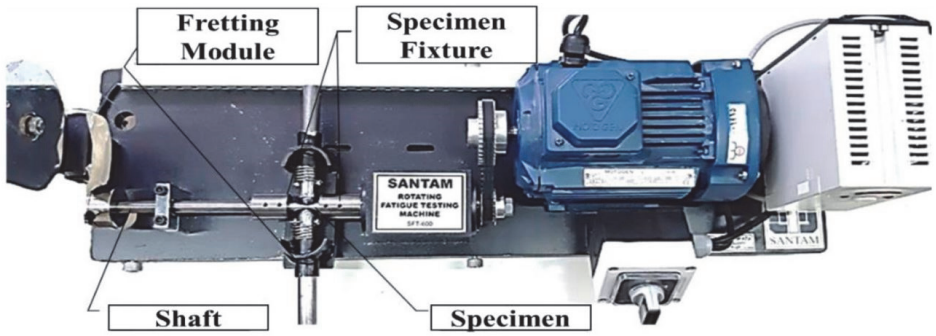

Figure 2: The rotational stress-controlled fatigue testing machine under bending loads with a fretting module [17].

Modeling techniques

Pearson's correlation coefficient is described to measure the linear relationship between variables to predict the value of one attribute based on another. In order to calculate the Pearson correlation coefficient between two variables (a, b), The following equation can be utilized [22]:

$$p(a,b)=\frac{E(a,b)}{\sigma_a\sigma_b} \tag{1}$$

where $P(a,b)$ represents the Pearson correlation coefficient between a and b, $E(a,b)$ denotes cross correlation, in addition to σ_a^2 and σ_b^2 are variances of a and b.

Shapely additive explanations (SHAP) values consumption is a method grounded in cooperative game theory to model interpretability [23].
Eqn. (2) can be utilized to determine SHAP values (φ_i) for each feature [24], as follows,

$$\varphi_i = \sum_{S \subseteq F/\{i\}} \frac{|S|!(|F|!-|S|-1)!}{|F|!}\left[f_{S\cup\{i\}}\left(x_{S\cup\{i\}}\right) - f_s\left(x_a\right)\right] \tag{2}$$

where F represents the model with all of its including features, S is a specific subset of the model, $S \cup \{i\}$ denotes the union of S and every single feature (i feature), as well as the model prediction including i feature is represented by $f_{s\cup\{i\}}\left(x_{s\cup\{i\}}\right)$, by contrast, $f_s\left(x_s\right)$ is prediction without i feature consideration, moreover predicted value from all features can be obtained by [24],

$$\hat{y} = \hat{y}_0 + \sum_{i=1}^{n} \varphi_i \tag{3}$$

where $\hat{y}$ represents the estimated value, while $\hat{y}_0$ determines the prediction regardless of features impact. XGBoost is a scalable tree-boosting algorithm, which is very powerful and fast for applications in ML challenges. The operation of this algorithm builds decision trees one after the other and corrects the mistakes of the previous trees. Eqn. (4) represents the objective which is to minimize the regularization [25],

$$Obj = \sum_{i=1}^{n} l\left(y_i, \hat{y}_i\right) + \sum_{j=1}^{K} \Omega\left(f_k\right) \tag{4}$$

where $l\left(y_i, \widehat{y_i}\right)$ presents the discrepancy between the actual and predicted values, $\Omega(ff)$ and K are determined as regularization terms and additive numbers of trees, respectively.
RF is a supervised learning algorithm. RF has appeared as a versatile method for classification and regression problems, as well as it integrates weak classifiers to provide optimal outcomes for complex tasks [26]. Random forest builds a collection of J number of decision trees; consequently, the overall prediction for input x, as well as the prediction for the j-th decision tree for input x, can be demonstrated as $f(x)$ and $h_j(x)$, respectively, in the following equation [27].

$$f(x) = \frac{1}{J}\sum_{j=1}^{J} h_j(x) \tag{5}$$

SVR belongs to the category of supervised ML techniques. Moreover, the effective proficiency of the generalization is one of its distinguishing features [28]. The SVR prediction target for a given input x represents $f(x)$, and it can be calculated using the following equation [29]:

$$y = w\varnothing(x) + b \tag{6}$$

where w represents the weight vector, $\varnothing(x)$ denotes the feature mapping of the input x, and b is the bias term.
Nonlinear regression modeling (NRM) represents a type of statistical regression. This method analyzes the relationship between dependent parameters and one or more independent parameters when they do not follow a straight-line pattern. By contrast, LRM assumes a linear combination of input features. The target variable, as the NRM model, is employed as the following equation:

$$y = f(x,\theta) + \varepsilon \tag{7}$$

where y represents the target variable, x is the input feature, θ denotes nonlinear regression parameters, and $f(\theta,x)$ is the prediction function [30].

Hyperparameter tuning and data splitting

In ML, hyperparameters are external configuration settings that are not learned from the data but are set prior to the training process. They play a crucial role in determining the performance of an ML model and are often tuned through a process called hyperparameter tuning [31]. In other words, fine-tuning hyperparameters can control the ML algorithm to prevent model overfitting, resulting in improved accuracy in both training and testing datasets. The hyperparameters for XGBoost, and RF were chosen from the literature [31], and the grid search cross-validation method was utilized as one of the common hyperparameter tuning methods for the present work. Moreover, to choose the best kernel function, linear kernel function, radial basis kernel function, polynomial kernel function, and sigmoid kernel function were utilized to train the kernel-based algorithms, and the grid search cross-validation method was employed to find the best kernel constants.

Before evaluating the performance of ML methods, the data were split into 20% and 80%, representing the testing and training subsets, respectively. The metrics (R^2 and *RMSE*), which will be explained in the next section, were obtained by changing the random state of the models 20 times. The reported metrics in this work are the average values obtained from these 20 runs. Tab. 2 demonstrates the number of data points, training data percentage, and testing data percentage utilized in the results of this paper. Furthermore, the best hyperparameters in this work represent the models with the highest training score and lowest score variation between training and testing data.

Figure/ Table	Total number of data points	Training data percentage	Testing data percentage
Tabs. 3, and 4	147	80%	20%
Figs. 4, 5, 6, 7, 8, and 9	147	100%	0

Table 2: The number of data points, training, and testing percentages of the data in the results of the paper.

Modeling evaluation

The effectiveness of prediction in modeling can be evaluated by the root mean square error (*RMSE*), the coefficient of determination (R^2), as well as the scatter band, which provides a valuable representation for visualizing a factor that encompasses the entire dataset of experimental lifetimes in comparison to the predicted values [32].

Briefly, a low *RMSE* indicates that the model's predictions are, on average, close to the actual values in the dataset. In contrast, a high *RMSE* suggests that the model predictions deviate significantly from the actual values. Eqn. (8) represents the *RMSE* value [24].

$$RMSE=\sqrt{\frac{1}{n}\sum_{i=1}^{n}\left(Y_{actual}-Y_{predicted}\right)} \tag{8}$$

where Y_{actual} represents the experimental value of fatigue lifetime in the present work, $Y_{predicted}$ denotes the estimated fatigue lifetime, and n is the number of samples.

Basically, R^2 ranges from 0% to 100%. A higher value of R^2 represents strong fitting to the data, while a value near 0% indicates poor fitting. However, a negative value signifies that the model fails to capture any variability in the dependent variable. Eqn. (9) denotes R^2 value [9].

$$R^2=1-\frac{\sum_{i=1}^{n}\left(Y_{actual}-Y_{predicted}\right)}{\sum_{i=1}^{n}\left(Y_{actual}-\overline{Y}_{predicted}\right)} \tag{9}$$

in which, Y_{actual} represents the experimental values of fatigue lifetime in the current study, $Y_{predicted}$ denotes the estimated fatigue lifetime, $\overline{Y}_{actual}$ illustrates the average value of fatigue lifetime based on the experimental dataset, and n is number of samples.

Scatter band plots depict actual and predicted values using a logarithmic scale for the axes. The line y=x symbolizes strong accuracy in modeling, and the scatter band values correspond to the slopes of lines that encompass the data points. A narrower scatter band suggests higher accuracy, indicating minimal deviation of the data from the y=x line [32].

RESULTS AND DISCUSSION

Selecting an optimal machine-learning algorithm

This section compares different ML approaches to evaluate their accuracy in predicting both the fatigue lifetime and the logarithm of the fatigue lifetime. In addition, the Pearson correlation matrix is commonly used as a simplified non-machine learning way to do sensitivity analysis on the mentioned dataset.

Tab. 3 presents comparison results for various ML techniques, providing mean R^2 and mean *RMSE* for estimating the logarithmic value of fatigue lifetime in both training and testing sets. The results in this table indicate a close alignment of mean metrics between the testing and training sets. Notably, XGBoost demonstrates the highest accuracy in predicting the logarithm of fatigue lifetime. However, despite its overall effectiveness compared to other methods, Tab. 4 reveals that XGBoost does not exhibit robust accuracy in estimating the testing values of fatigue lifetimes, as indicated by a mean R^2 value of 39% for the testing sets.

Based on the information provided, Fig. 3 presents the Pearson correlation between variables for fatigue lifetime and its logarithm. The results suggested that there was an insignificant correlation between the lubrication and the target variable. Specifically, the lubrication had a positive effect on the logarithmic value of fatigue lifetimes but a negative effect on the modeled fatigue lifetimes. These results aligned with the previous regression research [17]. Moreover, in the logarithmic model, the coloration coefficient between heat treatment and the logarithmic value of fatigue life was +0.32, indicating a more potent relationship than in the regular model, where it was +0.06.

Models	Hyperparameters	Mean R^2 (%)		Mean RMSE	
		Training	Testing	Training	Testing
XGBoost	n_estimators=100 max_depth=3 learning_rate=0.2 subsample=1.0 reg_lambda=1 colsample_bytree=0.6	**90.09**	**84.95**	**0.25**	**0.31**
RF	max_depth= 5 max_features= 'log2' min_samples_leaf= 1	87.59	80.79	0.28	0.36
SVM	Kernel='linear' C=10	78.12	74.17	0.37	0.42
NRM	alpha=1 Kernel='poly' degree=3	89.83	80.66	0.25	0.35
LM	-	78.86	75.00	0.37	0.41

Note: The **bold** value means the superior achievement.

Table 3: The accuracy for ML-based modeling of the logarithm value of fatigue lifetimes.

Fig. 4 (a) illustrates the difference between fatigue lifetime and estimated fatigue lifetime for different ML algorithms. Moreover, Fig. 4 (b) depicts the difference between the experimental logarithm value of fatigue lifetime and the estimated logarithm value of fatigue lifetime for different ML algorithms. In this boxplot, the best model is the one with the lowest error from zero. Therefore, in both figures, XGBoost has the lowest error from the zero value. Comparing the differences between estimated values and actual values for the target variable using a box plot, it becomes evident that XGBoost exhibits superiority over RF and SVR methods [12,33]. Moreover, the SVR results were the worst method in Fig. 4. As an agreement, Zhu et al. [30] indicated that the support vector techniques had lower R^2 values and higher RMSE compared to RF, for the high-cycle fatigue prediction of titanium alloys used in aero-engines.

Models	Hyperparameters	Mean R^2 (%)		Mean *RMSE*	
		Training	Testing	Training	Testing
XGBoost	n_estimators=100 max_depth=7 learning_rate=0.03 subsample=1.0 reg_lambda=1 colsample_bytree=0.8	**63.68**	**39.00**	**108528.67**	**156422.97**
RF	max_depth= 7 max_features='log2' min_samples_leaf= 3	54.88	33.09	121085.32	161984.83
SVM	Kernel='linear' C=10	0.76	-3.69	179868.89	21300.34
NRM	alpha=1 Kernel='rbf' gamma=0.1	61.62	37.76	111648.85	156899.54
LM	-	35.09	-31.19	145450.26	180328.61

Note: The **bold** value means the superior achievement.

Table 4: The accuracy for ML-based modeling of the fatigue lifetimes

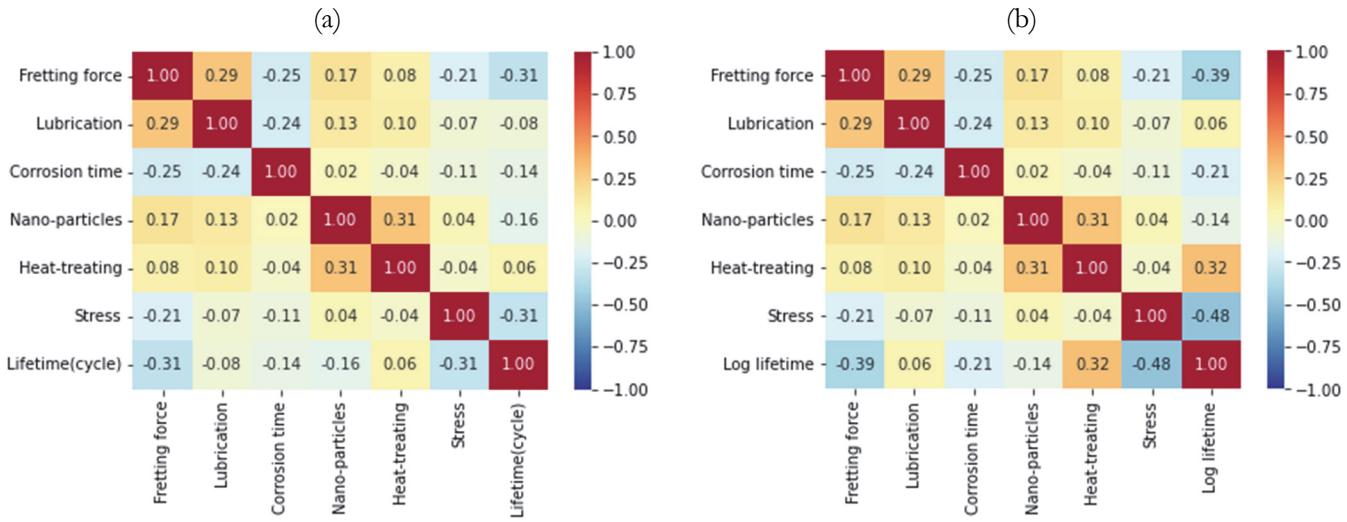

Figure 3: The Pearson correlation matrix, ranging from -1 to +1, illustrates the correlation between variables and the target for (a) fatigue lifetimes and other unchanged variables, and (b) the logarithmic value of fatigue lifetimes and other unchanged variables.

To compare the accuracy of fatigue lifetime modeling and the logarithmic value of fatigue lifetimes with XGBoost modeling, Fig. 5 represents the scatter bands for both of them. The fatigue lifetimes had a scatter band of ±8 for 95% of data points, while the scatter band for the logarithmic value of fatigue lifetimes was ±1.25, covering all data points. Thus, the logarithmic values of the fatigue lifetime model demonstrated a higher accuracy. Comparing these results with the literature, it is essential to mention that the scatter band for regression modeling of the logarithmic value of fatigue lifetime estimation was approximately ±1.5 when using the same dataset as the literature [17]. This suggests that XGBoost demonstrates its superiority over traditional regression modeling in this context. Long et al. [35] showed that the scatter band was narrower (less than ±2.0) when using boosting methods, compared to the support vector techniques in predicting the logarithmic values of low-cycle fatigue lifetimes in lead-free solders [35], compared to the results through the high-cycle fatigue regime in this work. Unlink that work, Hao et al. [36] illustrated that physics-informed ML techniques had proper simplicity and high accuracy for estimating the notch fatigue lifetime of polycrystalline alloys. They demonstrated that the accuracy of RF was higher than XGBoost. Moreover, the SVR accuracy was lower than others, which was in agreement with the results of the present work for aluminum alloys.

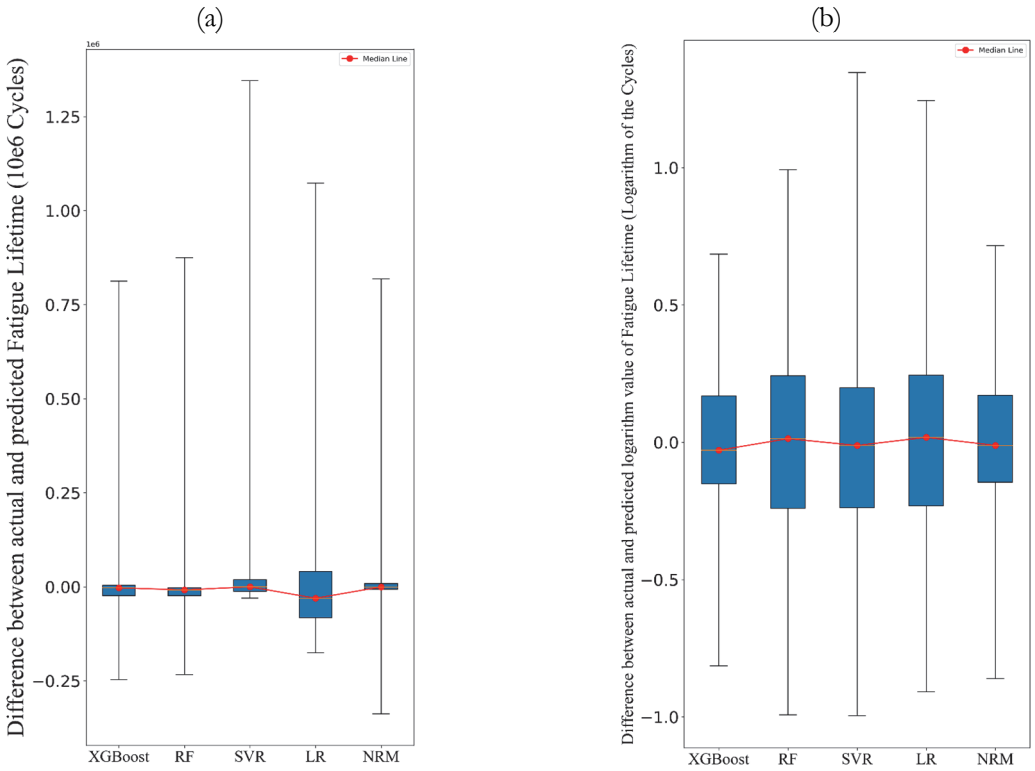

Figure 4: Difference between trained experimental target value and estimated target value for different ML methods: (a) Target: fatigue lifetime (b) Target: logarithm value of fatigue lifetime.

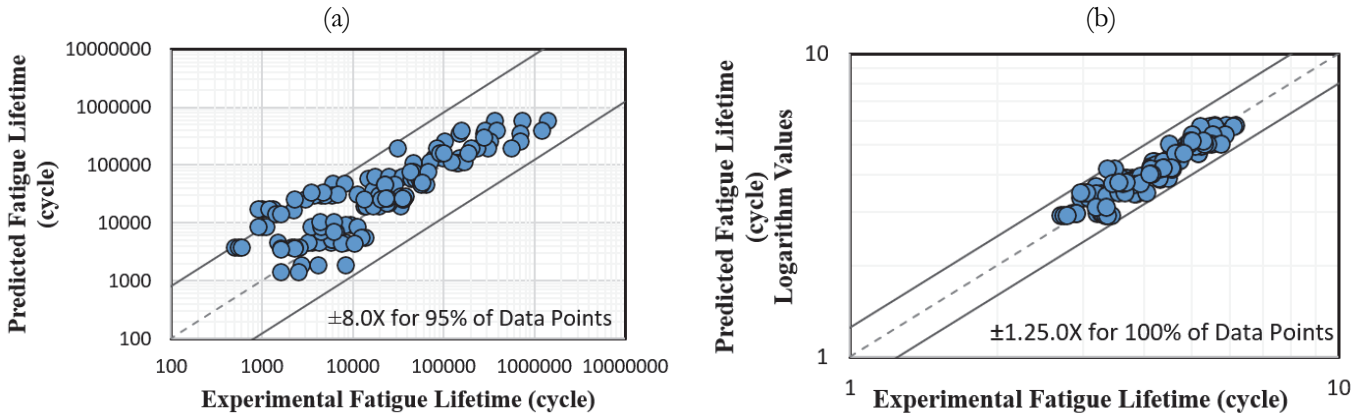

Figure 5: The scatter band plots comparing experimental data to predicted values, generated by training the entire dataset using XGBoost with mentioned hyperparameters for (a) fatigue lifetime modeling and (b) modeling the logarithmic values of fatigue lifetimes.

SHAP analysis of the XGBoost model

This section presents the results of the SHAP analysis conducted on the XGBoost model trained to predict the logarithm value of fatigue lifetime. Before this analysis, the best model for predicting fatigue lifetime and its logarithm was determined, and it was found that the algorithm performed better when trained with the logarithm value of fatigue lifetime. This analysis demonstrates the impact of variables on the logarithmic value of fatigue lifetime.

Fig. 6 illustrates a one-dimensional scatter plot, displaying individual feature contributions to model predictions. The fretting force factor had the most significant contribution to the estimation of the target, while the lubrication had the lowest contribution. Moreover, several prior studies, including references [11, 12, 15, 24, 25, 33], have employed a similar approach to interpreting feature significance for estimating the target and visualizing the distribution of SHAP values, as seen in the

beeswarm diagram presented in Fig. 7. Based on Eqns. (2) and (3), each specified feature in a sample has a SHAP value that collects to the regardless of the feature predicting value of the target. In Fig. 6, the SHAP value distribution of each feature in the entire dataset is demonstrated. However, Fig. 7 depicts the mean absolute SHAP value among all the data. This finding can aid in classifying each feature by showcasing the average impact of each feature on fatigue lifetime, as shown in Fig. 7(a), and the logarithm of fatigue lifetimes, as shown in Fig. 7b), serving as the target of the modeling process. Meanwhile, Fig. 7 displays the ranking of variable impacts on model predictions. According to the sensitivity analysis in the regression model [17], stress was identified as the most influential variable in predicting the logarithmic value of fatigue lifetimes. In contrast, in the SHAP modeling, the fretting force was recognized as the dominant factor. Chelgani et al. [12] used a method similar to that shown in Fig. 6 to represent the correlation between features and the target variable, as well as to rank the features based on SHAP values and the XGBoost algorithm. In the bar plots in Fig. 7, the color is sensitive to changes in the features and their consequences changing the SHAP values, not positive and negative signs of the SHAP values [12,33]. The difference, seen in the bar plots between Figs. 7 (a) and (b) for the lubrication, is also evident in Figs. 3 (a) and (b) for the lubrication, illustrating the sensitivity of regression modeling and XGBoost to logarithmic transformations [37].

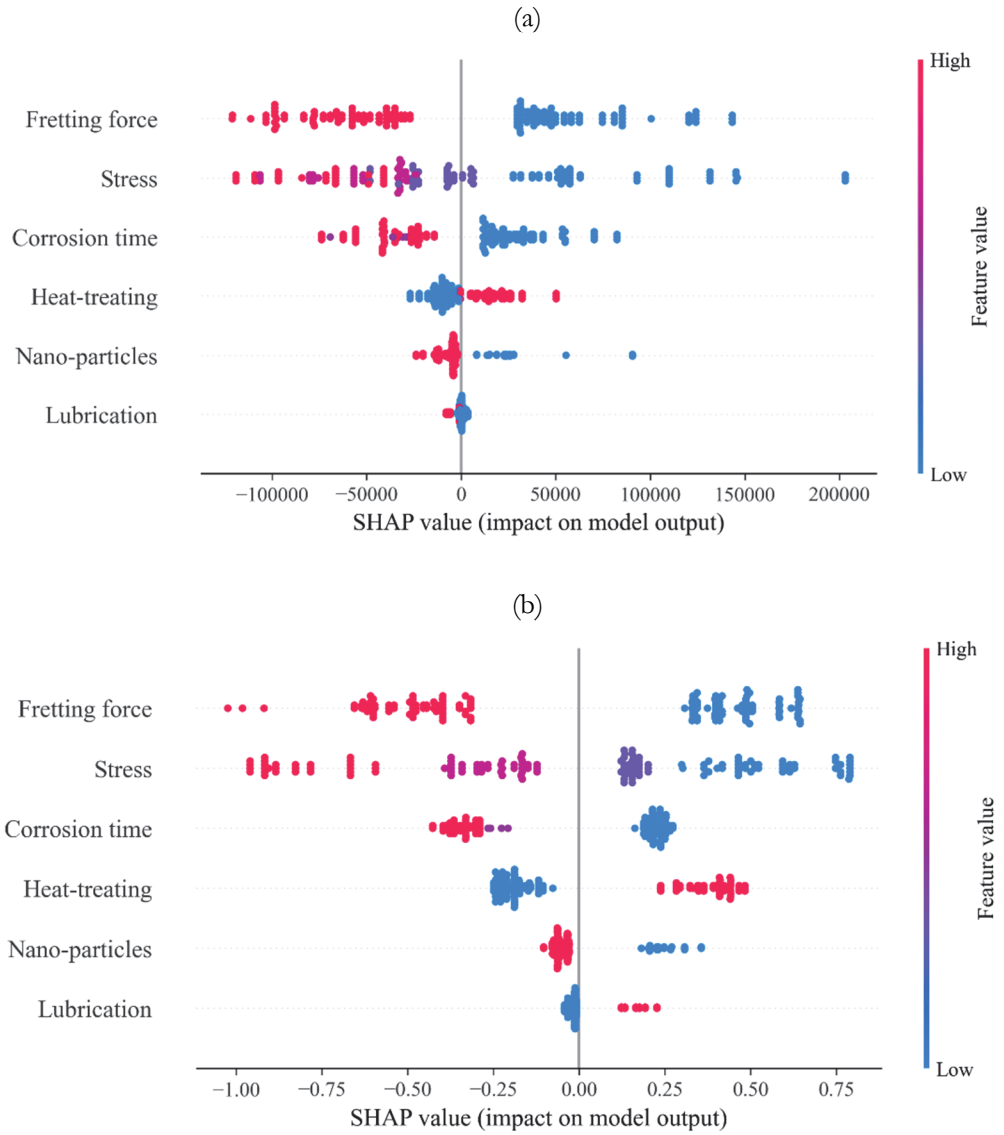

Figure 6: The beeswarm diagram illustrates the SHAP distribution among the variables in all of the trained samples using XGBoost for (a) fatigue lifetimes and (b) the logarithmic value of fatigue lifetimes.

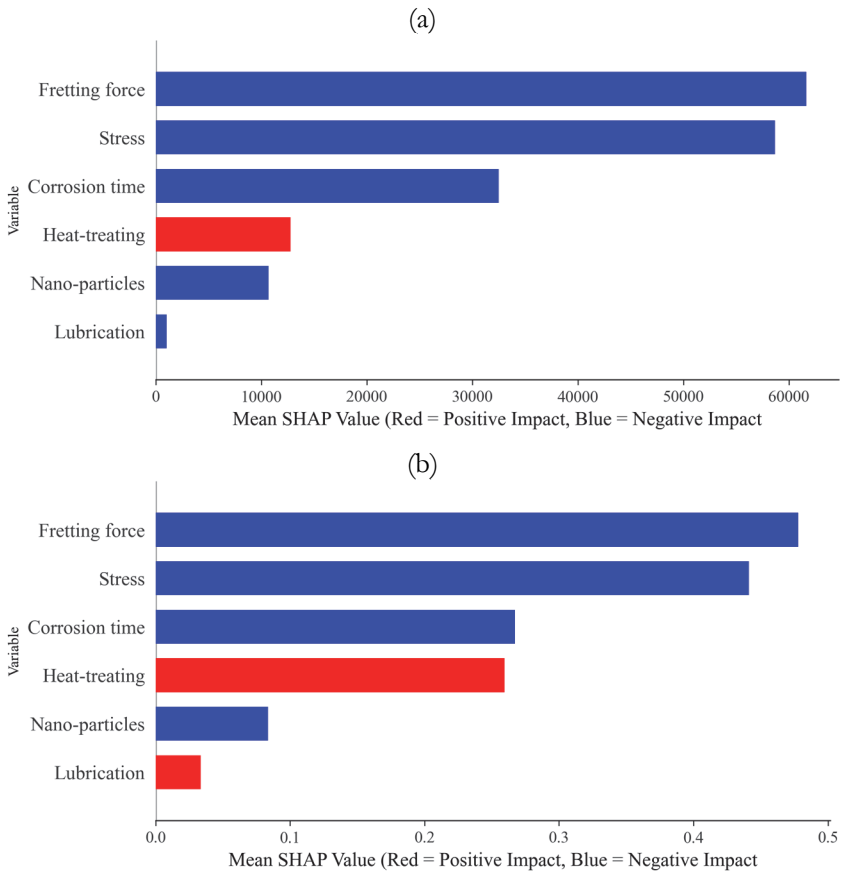

Figure 7: The mean SHAP value of different inputs modeled with XGBoost using all of the samples as trained data for (a) fatigue lifetimes modeling and (b) the logarithmic value of fatigue lifetimes modeling.

To understand how an individual variable affects the target, Fig. 8 illustrates the SHAP values of that variable across all samples for different parameter values. In Fig. 8, another variable, such as stress, was employed to color the samples, illustrating the relationship between stress and other variables. The concentration of data points in Figs. 8 (c), (e), and (f) in scatter plots is noticeable in certain regions linked to categorical features. Additionally, the distribution of various values among these features was not uniform across samples, consistent with previous research on categorical features [33].

Based on the points mentioned in Modeling Techniques Section, SHAP values rely on the game theory. According to Eqn. (3), each sample, after interpretation with SHAP values, is assigned a prediction value regardless of other features. Furthermore, each feature has a corresponding SHAP value, and these values are aggregated for predictions. If there is no interaction between variables, a figure like Fig. 8 can provide readers with an overall estimation of the logarithm value of fatigue lifetimes for their assumed variables, without resorting to complex computational methods. To support this claim, considering Fig. 8(a), which illustrates how the SHAP value for estimating the logarithm value of fatigue lifetimes changes with the fretting force. For instance, when the fretting force is zero, the SHAP value is approximately +0.5, while at +10 N, it becomes about -0.5. Notably, the SHAP value decreases further to about -1 when the fretting force increases from 10 N to 15 N. However, the SHAP value does not significantly change from 15 N to 20 N at low stress levels. This observation highlights the non-linear behavior of the fretting force in the estimation of the logarithm value of fatigue lifetimes. Moreover, the interpretation of SHAP values for corrosion time in Fig. 8(b) demonstrates that when time changes from zero to 100 hrs, the SHAP values for corrosion time approximately change from 0.2 to -0.2. While the change in the corrosion time from 100 hrs to 200 hrs is observed, the SHAP values for corrosion time change from approximately -0.2 to -0.4. This finding illustrates that there is non-linearity in the behavior of the distribution of SHAP values for the corrosion time when changing from zero to 100 hrs, while the time changed from 100 hrs to 200 hrs exhibits linearity, as can be concluded from this figure. These findings consistently hold across all sections of Fig. 8. Through the analysis of SHAP values, the utilization of the Pearson correlation matrix, and an understanding of the physics of the dataset variables, it becomes evident that there is no interaction between variables. Therefore, based on the game theory, the overall change in the estimated logarithm value of fatigue lifetimes can be derived from this figure for each specified sample.

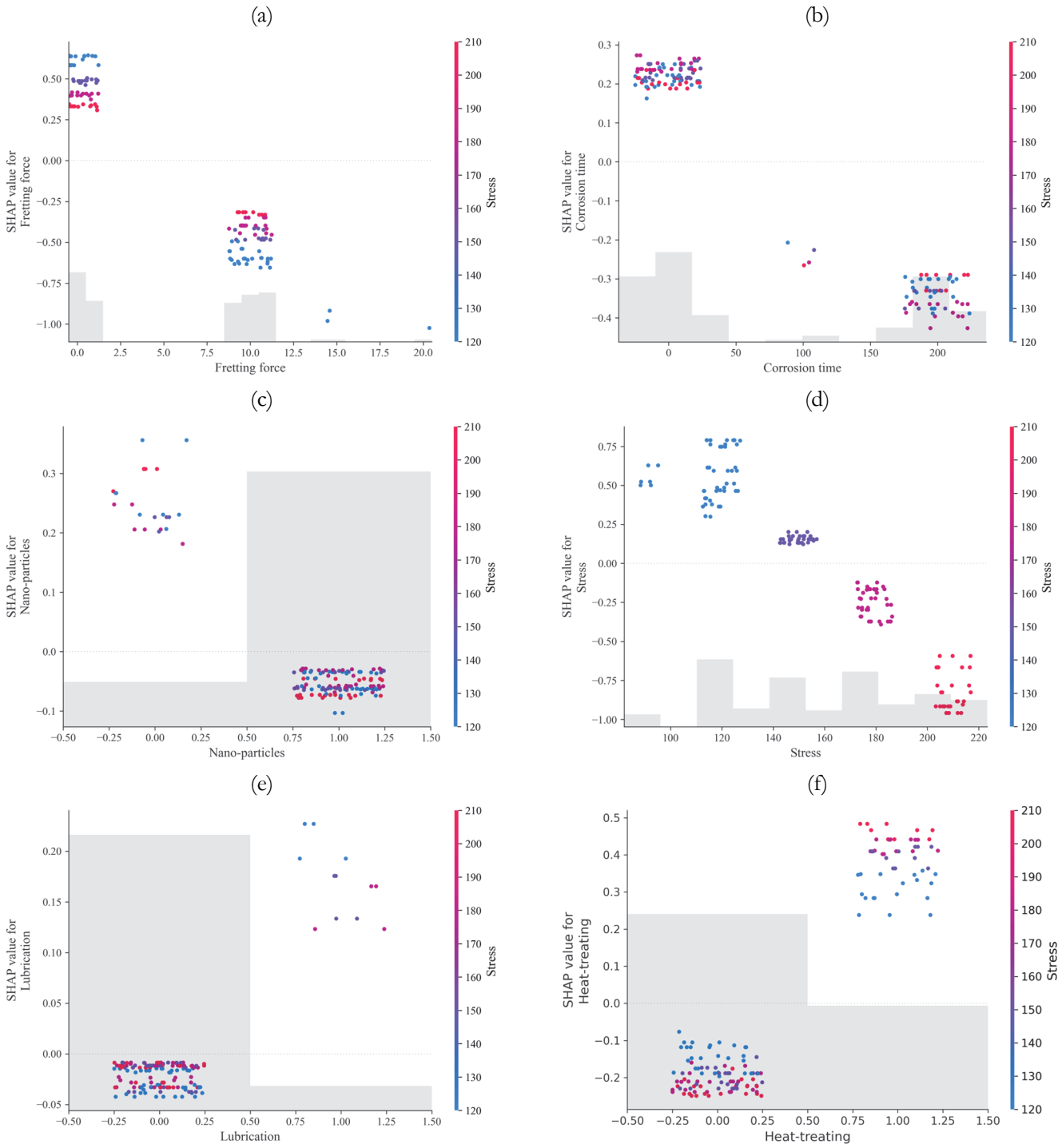

Figure 8: The histogram and scatter plot for the SHAP values of the logarithmic value of fatigue lifetimes modeling with XGBoost using all of the samples as trained data for different variables: (a) the fretting force, (b) the corrosion time, (c) nano-particles, (d) the stress, (e) the lubrication, and (f) the heat treatment.

To illustrate how the game theory, in conjunction with SHAP values, can provide an overview for estimating the logarithm value of fatigue lifetimes, Fig. 9 showcases samples numbered 20 and 65 from the experimental dataset. In this figure, each feature is assigned a specified SHAP value, where $f(x)$ represents the estimated logarithm value of fatigue lifetimes and $E[f(x)]$ denotes the predicted logarithm of fatigue lifetimes irrespective of features. Notably, $E[f(x)]$ remains constant across all samples, equivalent to $\hat{y}_0$ in Eqn. (3). The collected SHAP values for each specified sample are

represented by $\sum_{i=1}^{n} \varnothing_i$. Therefore, in each specified sample, the collected SHAP values can be summed to 4.128 to obtain an estimated fatigue lifetime based on the assumed inputs.

In future research, it would be beneficial to explore physics-based models and examine the influence of physical characteristics derived from feature engineering methods on fatigue lifetimes.

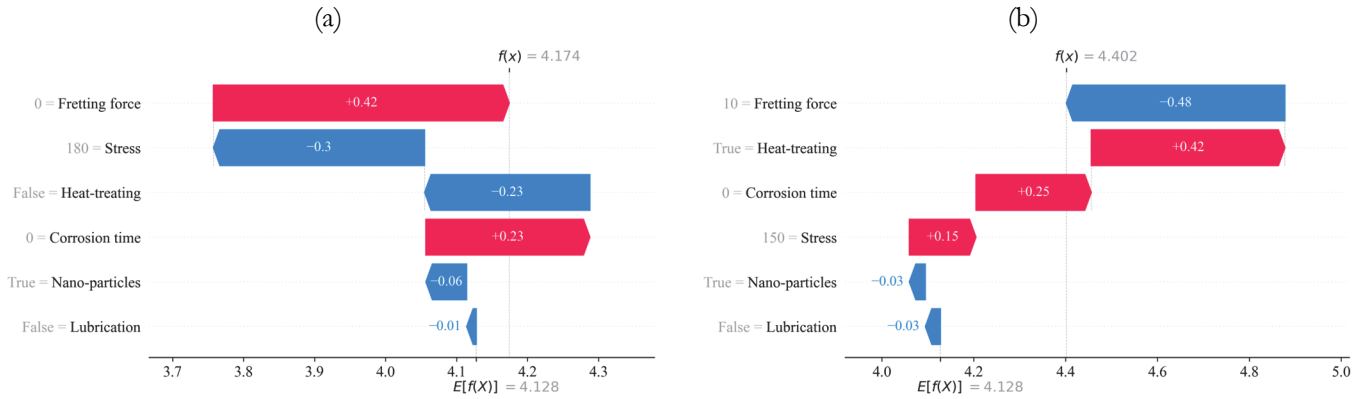

Figure 9: Waterfall plots for the XGBoost estimating of logarithm value of fatigue lifetime for two different samples using game theory and SHAP values: (a) Sample number of 20 from the experimental dataset, (b) Sample number of 65 from the experimental dataset.

CONCLUSIONS

This study focused on utilizing multiple ML models to predict the fatigue lifetime of various specimens made from an aluminum-silicon alloy, commonly used in engine pistons. Additionally, the prediction considered the impacts of various inputs on the fatigue lifetime. The modeling process produced the subsequent results, as follows,

- The top-performing model for predicting fatigue lifetimes and their logarithmic values was XGBoost. The evaluation of algorithms was compared in training and testing sets with two metrics, determination coefficient (R^2), and root mean square error (RMSE). The mean metrics for predicting the logarithmic value of fatigue lifetime with testing sets were notably strong for XGBoost, with a mean *RMSE* of 0.31 and a mean R^2 of 84.5% among 20 different testing sets. However, the XGBoost model was not accurate in predicting fatigue lifetime values with the same testing sets, as evidenced by a mean *RMSE* of 156,422.97 and a mean R^2 of 39%.
- From the scatter band, as another modeling evaluation, it illustrates, based on assumed hyperparameters, that the scatter band value for the fatigue lifetime prediction with XGBoost was ±8 (covering 95% of the data) and ±1.25 (for all data) for the logarithm of fatigue lifetimes with XGBoost. This indicates the accuracy of the logarithmic value of fatigue lifetimes. It is concluded that it is better to take the logarithm of the fatigue lifetime and then train it in machine learning (ML) models.
- The estimated baseline value of the logarithm of fatigue lifetimes based on the game theory is reported with a value of 4.128. To predict a logarithmic value of fatigue lifetimes with an assumed input, the reader can derive approximate SHAP values for each feature one by one and sum them with 4.128.
- In the regression analysis, the stress and fretting force, among others, were significant variables. However, the SHAP analysis demonstrated that fretting force was the most essential variable.
- According to the SHAP values, the fretting force had the most significant impact, while lubrication had the slightest significant influence on the fatigue lifetime and its logarithms.

DATA AVAILABILITY

The raw experimental data are available at M. Azadi and M.S.A. Parast, "HCF testing raw data on piston aluminum alloys", Mendeley Data, V2, 2021,
DOI: 10.17632/cghj3vw67j.2 (https://data.mendeley.com/datasets/cghj3vw67j/2).

REFERENCES

[1] Yao, Z. and Li, W. (2020). Microstructure and thermal analysis of APS nano PYSZ coated aluminum alloy piston. Journal of Alloys and Compounds, 812, 152162. DOI: 10.1016/j.jallcom.2019.152162.

[2] Skryabin, M.L. and Grebnev, A. (2020). Promising methods for strengthening piston aluminum alloys of heat engines. Journal of Physics: Conference Series, 2020. IOP Publishing, 052052. DOI: 10.1088/1742-6596/1515/5/052052.

[3] Alshalal, I. Al-Zuhairi, H. M. I. Abtan, A. A. Rasheed, M. and Asmail, M. K. (2023). Characterization of wear and fatigue behavior of aluminum piston alloy using alumina nanoparticles. Journal of the Mechanical Behavior of Materials, 32 (1), 20220280. DOI: 10.1515/jmbm-2022-0280.

[4] Sun, G.Q. and Shang, D.G. (2010). Prediction of fatigue lifetime under multiaxial cyclic loading using finite element analysis. Materials & Design, 31, pp. 126-133. DOI: 10.1016/j.matdes.2009.06.046.

[5] Sivachev, S. and Myagkov, L. (2020) Thermomechanical fatigue analysis of diesel engine piston: finite element simulation and lifetime prediction technique. Proceedings of the 5th International Conference on Industrial Engineering (ICIE 2019) I 5, pp. 109-117. DOI: 10.1007/978-3-030-22041-9_13.

[6] Castillo, E. and Fernandez-Canteli, A. (2001). A general regression model for lifetime evaluation and prediction. International Journal of Fracture, 107, pp. 117-137. DOI: 10.1023/A:1007624803955

[7] Pierce, S.G. Worden, K. and Bezazi, A. (2008). Uncertainty analysis of a neural network used for fatigue lifetime prediction. Mechanical Systems and Signal Processing, 22 (6), pp. 1395-1411. DOI: 10.1016/j.ymssp.2007.12.004.

[8] Avoledo, E. Tognan, A. and Salvati, E. (2023). Quantification of uncertainty in a defect-based Physics-Informed Neural Network for fatigue evaluation and insights on influencing factors. Engineering Fracture Mechanics, 292, 109595. DOI: 10.1016/j.engfracmech.2023.109595

[9] Xiong, J. Shi, S.Q. and Zhang, T.Y. (2021). Machine learning of phases and mechanical properties in complex concentrated alloys. Journal of Materials Science & Technology, 87, pp. 133-142. DOI: 10.1016/j.jmst.2021.01.054.

[10] Durodola, J. F. (2022). Machine learning for design, phase transformation and mechanical properties of alloys. Progress in Materials Science, 123, 100797. DOI: 10.1016/j.pmatsci.2021.100797

[11] Wang, D. Thunell, S. Lindberg, U. Jiang, L. Trygg, J. and Tysklind, M. (2022). Towards better process management in wastewater treatment plants: Process analytics based on SHAP values for tree-based machine learning methods. Journal of Environmental Management, 301, 113941. DOI: 10.1016/j.jenvman.2021.113941

[12] Chelgani, S. C. Nasiri, H. and Alidokht, M. (2021). Interpretable modeling of metallurgical responses for an industrial coal column flotation circuit by XGBoost and SHAP-A "conscious-lab" development. International Journal of Mining Science and Technology, 31, pp. 1135-1144. DOI: 10.1016/j.ijmst.2021.10.006

[13] Abdullatef, M. S. Alirezzaq, N. and Hasan, M.M. (2016). Prediction fatigue life of aluminum alloy 7075 T73 using neural networks and neuro-fuzzy models. Engineering and Technology Journal, 34 (2), pp. 272-283. DOI: 10.30684/etj.2016.112624

[14] Yasnii, O.P. Pastukh, O.A. Pyndus, Y. I. Lutsyk, N.S and Didych, I.S. (2018). Prediction of the diagrams of fatigue fracture of D16T aluminum alloy by the methods of machine learning. Materials Science, 54, pp. 333-338.

[15] DOI: 10.1007/s11003-018-0189-9.

[16] Lian, Z. Li, M. and Lu, W. (2022). Fatigue life prediction of aluminum alloy via knowledge-based machine learning. International Journal of Fatigue, 157, 106716. DOI: 10.1016/j.ijfatigue.2021.106716.

[17] Matin, M. and Azadi, M. (2023). A novel machine learning-based model for predicting of transition fatigue lifetime in piston aluminum alloys. Preprint in SSRN. Available at SSRN 4598611. DOI: 10.2139/ssrn.4598611.

[18] Azadi, M. and Parast, M. S. A. (2022). Data analysis of high-cycle fatigue testing on piston aluminum-silicon alloys under various conditions: Wear, lubrication, corrosion, nano-particles, heat-treating, and stress. Data in brief, 41, 107984. DOI: 10.1016/j.dib.2022.107984.

[19] Tognan, A. Patanè, A. Laurenti, L. and Salvati, E. (2024). A Bayesian defect-based physics-guided neural network model for probabilistic fatigue endurance limit evaluation. Computer Methods in Applied Mechanics and Engineering, 418, 116521. DOI: 10.1016/j.cma.2023.116521

[20] Salvati, E. Tognan, A. Laurenti, L. Pelegatti, M. and De Bona, F. (2022). A defect-based physics-informed machine learning framework for fatigue finite life prediction in additive manufacturing. Materials & Design, 222, 111089. DOI: 10.1016/j.matdes.2022.111089

[21] Zhu, S.P. Wang, L. Luo, C. Correia, J.A. De Jesus, A.M. Berto, F. and Wang, Q. (2023). Physics-informed machine learning and its structural integrity applications: state of the art. Philosophical Transactions of the Royal Society A, 381, 20220406. DOI: 10.1098/rsta.2022.0406

[22] Matin, M. and Azadi, M. (2023). The effect of training data ratio and normalizing on fatigue lifetime prediction of aluminum alloys with machine learning. International Journal of Engineering. Available at: https://www.ije.ir/article_186504.html
[23] Cohen, I. Huang, Y. Chen, J. Benesty, J. Benesty, J. Chen, J. Huang, Y. and Cohen, I. (2009). Pearson correlation coefficient. Noise reduction in speech processing, pp. 1-4. DOI: 10.1007/978-3-642-00296-0_5.
[24] Lundberg, S. M. and Lee, S. I. (2017). A unified approach to interpreting model predictions. Advances in neural information processing systems, 30. ISBN: 9781510860964.
[25] Wen, X., Xie, Y. Wu, L. and Jiang, L. (2021). Quantifying and comparing the effects of key risk factors on various types of roadway segment crashes with LightGBM and SHAP. Accident Analysis & Prevention, 159, 106261. DOI: 10.1016/j.aap.2021.106261.
[26] Meng, Y. Yang, N. Qian, Z. and Zhang, G. (2020). What makes an online review more helpful: an interpretation framework using XGBoost and SHAP values. Journal of Theoretical and Applied Electronic Commerce Research, 16, pp. 466-490. DOI: 10.3390/jtaer16030029.
[27] Biau, G. and Scornet, E. (2016). A random forest guided tour. Test, 25, 197-227. DOI: 10.1007/s11749-016-0481-7
[28] Cutler, A. Cutler, D. R. and Stevens, J. R. (2012). Random forests. Ensemble machine learning: Methods and applications, pp. 157-175. DOI: 10.1007/978-1-4419-9326-7_5.
[29] Huang, Q. Mao, J. and Liu, Y. An improved grid search algorithm of SVR parameters optimization. (2012). IEEE 14th International Conference on Communication Technology, pp. 1022-1026. DOI: 10.1109/ICCT.2012.6511415.
[30] Wu, C.H. Ho, J.M. and Lee, D.T. (2004). Travel-time prediction with support vector regression. IEEE transactions on intelligent transportation systems, 5, pp. 276-281. DOI: 10.1109/TITS.2004.837813.
[31] Ahmadi-Nedushan, B. (2012). Prediction of elastic modulus of normal and high strength concrete using ANFIS and optimal nonlinear regression models. Construction and Building Materials, 36, pp. 665-673. DOI: 10.1016/j.conbuildmat.2012.06.002
[32] Putatunda, S. and Rama, K. (2018). A comparative analysis of hyperopt as against other approaches for hyper-parameter optimization of XGBoost. Proceedings of the 2018 international conference on signal processing and machine learning, pp. 6-10. DOI: 10.1145/3297067.3297080.
[33] Azadi, M. Shahsavand, A. and Parast, M. S. A. (2022). Analyzing experimental data from reciprocating wear testing on piston aluminum alloys, with and without clay nano-particle reinforcement. Data in Brief, 45, 108766. DOI: 10.1016/j.dib.2022.108766
[34] Nasiri, H. Azadi, M. and Dadashi, A. (2023). Interpretable Extreme Gradient Boosting Machine Learning Model for Fatigue Lifetimes in 3D-Printed Polylactic Acid Biomaterials. Preprint in SSRN. Available at SSRN 4364418. DOI: 10.2139/ssrn.4364418
[35] Zhu, S. Zhang, Y. Chen, X. He, Y. and Xu, W. (2023). A multi-algorithm integration machine learning approach for high cycle fatigue prediction of a titanium alloy in aero-engine. Engineering Fracture Mechanics, 289, 109485. DOI: 10.1016/j.engfracmech.2023.109485
[36] Long, X. Lu, C. Su, Y. and Dai, Y. (2023). Machine learning framework for predicting the low cycle fatigue life of lead-free solders. Engineering Failure Analysis, 148, 107228. DOI: 10.1016/j.engfailanal.2023.107228
[37] Hao, W. Tan, L. Yang, X. Shi, D. Wang, M., Miao, G. and Fan, Y. (2023). A physics-informed machine learning approach for notch fatigue evaluation of alloys used in aerospace. International Journal of Fatigue, 170, 107536. DOI: 10.1016/j.ijfatigue.2023.107536
[38] Raudys, A. and Goldstein, E. (2022). Forecasting Detrended Volatility Risk and Financial Price Series Using LSTM Neural Networks and XGBoost Regressor. Journal of Risk and Financial Management, 15 (12), 602. DOI: 10.3390/jrfm15120602